Hindawi
Shock and Vibration
Volume 2019, Article ID 1934240, 14 pages
https://doi.org/10.1155/2019/1934240

Research Article

Grouting Defect Detection of Lapped Bar Connections Based on Impact-Echo Method

Yun-Lin Liu,[1] Jing-Jing Shi,[1] Jun-Qi Huang ,[2,3] Guang-Shuo Wei,[4] and Zhi-Xin Wu[4]

[1]*School of Civil Engineering, Anhui Jianzhu University, Hefei 230601, China*
[2]*School of Civil and Hydraulic Engineering, Hefei University of Technology, Hefei 230009, China*
[3]*Department of Civil and Environmental Engineering, The Hong Kong Polytechnic University, Hong Kong, China*
[4]*Anhui Institute of Building Research and Design, Hefei 230088, China*

Correspondence should be addressed to Jun-Qi Huang; junqihuang001@163.com

Received 20 May 2019; Revised 22 August 2019; Accepted 18 September 2019; Published 14 October 2019

Academic Editor: Mohammad Rafiee

Grouted lap-splice connections are widely used for connecting precast concrete components. Grouting defects in the connections significantly influence the structural performance of the whole connection, which leads to the need for grouting defect detection. In this study, the impact-echo (IE) method was used for detecting defects in grouted lap-splice connections. Grouted connections with different levels of artificial grout defects were prepared in a shear wall, and the IE method was used to measure the frequency response. In addition, finite element (FE) analysis based on ABAQUS was conducted to simulate the tests. Based on the validated FE model, a parametric study was conducted to investigate the effect of the depth of the grout hole on the amplitude spectrum. The results indicated that (1) the IE method offered a good potential for grouting defect detection in grouted lap-splice connections; (2) the proposed FE model could well predict the frequency response of the grouting hole; and (3) the measured frequency and amplitude of the grouting hole in an impact-echo test would be considerably influenced by the hole depth.

1. Introduction

Grouted lap-splice connections are typical in precast concrete structures, which result in easy construction compared with other connecting systems (e.g., grouted sleeves). Generally, during the construction process, the connecting steel bars are inserted into the precast concrete components that need to be connected initially. Thereafter, cement-based material (i.e., grout) is injected from the prepared hole (see "Grouting inlet" in Figure 1), and the connections are formed after the curing stage. Figure 1 shows the details of the grouted lap-splice connection.

Grouting quality directly affects the structural performance of the connected elements because it is the key part that connects two adjacent components together. If the grout contains large voids, the existing water and air inside the hole would cause corrosion of the connecting steel bars. Furthermore, it would influence the structural performance of the precast concrete components. In addition, defects in the grout will lead to stress concentration in the lapped bars, which results in a stress state that is inconsistent with the design and may affect the overall structural safety. Therefore, it is necessary to develop a method to detect defects in grouted lap-splice connections.

Nondestructive testing (NDT) techniques have been developed to evaluate the material properties and soundness of concrete elements since 1940s [1]. The impact-echo (IE) method is one of the NDT techniques for concrete flaw detection. The IE method is based on the propagation and reflection of stress waves induced by a short-duration mechanical impact [1–6]. The IE response is related to the material property, the geometry of the test specimen, boundary conditions, flaw size, and flaw location within the specimen [1–6]. Details of the working principle of the IE testing method are introduced in the following section.

In the 1980s, the IE method was adopted in the civil engineering field to detect flaws in concrete and masonry structures [1, 2]. Sansalone and Streett [2] provided guideline on how to use the IE method in practical engineering. The IE method has been used successfully to detect

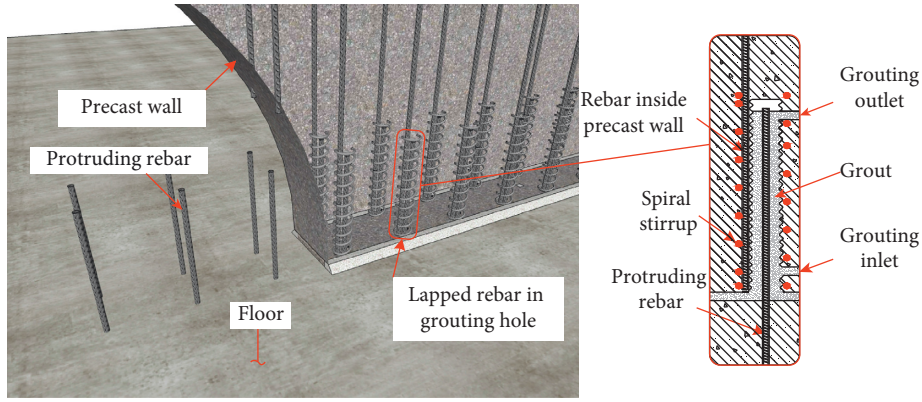

Figure 1: Reinforced mortar anchor lap connection.

flaws in various structural components, such as prestressed concrete slabs [6], reinforced concrete beams and columns [7], concrete blocks [8], epoxy-concrete interface [9], bridge decks [10], I-girders [11], tunnel linings [12], cavities around concrete sewage pipelines [13], prestressed concrete slabs [14], and grouting of prestressed concrete structural members [15–18].

Although research has been conducted in this field, there is a lack of information on the application of the IE method in defect detection of grouted lap-splice connections. Therefore, the objective of this study is to investigate whether the existing IE method could be used to detect grouting defects in grouted lap-splice connections of shear walls. For this purpose, a precast shear wall containing grouting holes with a series of artificial defects was used to investigate the applicability of the IE method. The frequency response of the grouted holes with different defect levels were determined and compared in detail. In addition, finite element (FE) analyses were conducted to simulate the test and a parametric study was conducted to investigate the effect of hole depth on the frequency response.

2. Theory and Test System of the Impact-Echo (IE) Method

2.1. Theory of the IE Method. The IE method is a NDT technique that incorporates the principle of low-frequency transient stress wave propagation. The principle of the IE technique is illustrated in Figure 2, in which T is the distance from the internal defect to the top plate surface and Δt is the time when the P-wave first arrives at the signal receiving point. A small steel ball is used to impact the specimen surface, which generates stress waves that propagate through the test specimen. Three types of waves are generated, which are named as P-, S- and R-waves. The P-wave and S-wave are associated with particle motion parallel and perpendicular to the propagation direction, respectively. The R-wave (also known as Rayleigh wave) is a surface wave that travels along the solid surface. In the IE method, the measured displacement response is mainly

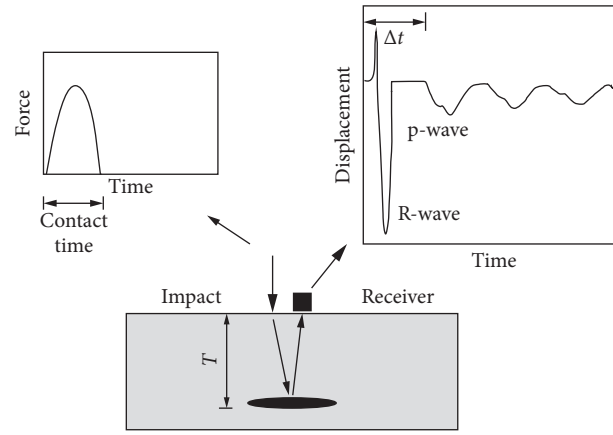

Figure 2: Principle of the impact-echo method [1].

influenced by the P-wave, owing to the close location of the sensor and impact point [1, 2]. Reflection, refraction, and diffraction would occur when these waves encounter interfaces between materials with different acoustic impedances.

The sensor responds to the arrival of reflected waves, and the recorded time domain signals are transformed into the frequency domain using the fast Fourier transform (FFT) technique. The frequency with peak amplitude in the obtained spectrum represents the dominant frequency in the waveform. This dominant frequency, also known as the thickness frequency, can be estimated as

$$f = \frac{\beta K}{n} \frac{V_p}{T}, \tag{1}$$

where K is a geometric correction factor that is determined by the geometrical shape of the structure [3]; n is a constant factor either equal to 2 or 4 depending on the acoustic impedances [3]; β is an empirical correction factor which has a value of 0.96 [1, 2] or 0.95 [4, 5]; and V_p is the P-wave speed and is calculated through $V_p = \{E(1-\nu)/[\rho(1+\nu)(1-2\nu)]\}^{0.5}$, where E, ρ, and ν are the elastic modulus, density, and Poisson's ratio of the test object, respectively.

For the precast shear wall in this study, K, β, and n are equal to 1.0, 0.96, and 2.0, respectively [1, 2].

2.2. IE Test

2.2.1. Introduction. An IE test system mainly includes three components: a small steel ball, a transducer, and a waveform analyzer. The frequency content of the stress pulse is governed by the impact contact time, and most of the energy in a stress pulse exists in a frequency of 0 to $1.5/t_c$ (t_c is the contact time). With a decrease of the contact time, the frequency range would be increased. With shorter contact times, smaller defects can be discerned and shallower depths can be measured. However, the amplitude of each component frequency would be lowered, which decreases the penetrating ability of the stress waves [2]. As the contact time is a linear function of the ball diameter and has a very weak dependence on the kinetic energy at impact [2], the selection of the impact source significantly influences the results of an IE test. In this study, the impactor was a 6 mm steel sphere, which has a contact time of approximately 25 μs with the concrete [2].

2.2.2. Application of the IE Test System. Whether a void in a slab or wall can be detected mainly depends on its lateral dimensions (l in Figure 3), depth (d in Figure 3), and the contact time [1]. If $l > (1/4)d$, the presence of the flaw can be detected. If $l > (1/3)d$, the flaw depth can be measured. If $l > 1.5\,d$, the flaw behaves as an infinite boundary [1]. If $(1/3) < (l/d) < 1.5$ (shaded region shown in Figure 3), the amplitude spectrum typically has two peaks: a higher frequency peak corresponding to the depth of the flaw, which can be obtained only if the impact contact time is sufficiently short, and a lower frequency peak that would be lower than the thickness frequency of the unflawed plate.

Figure 4 shows a typical precast shear wall panel as an example to clarify the above rules. In engineering practice, the grouting hole could be at different locations as shown in the figure. Given a grouting hole with the diameter of 35 mm, the hole depth in Figures 4(a) and 4(b) can be measured because the values of l/d are 0.7 and 0.467, respectively, which fall within the shaded region of Figure 3. If the grouting hole is located at the midthickness of the wall (Figure 4(c)), the depth could also be measured since l/d is 0.35 in this case. However, in the case of Figures 4(d) and 4(e), the l/d values are 0.28 and 0.233, which are lower than 1/3 and the depth cannot be measured. Furthermore, the flaw in the case of Figure 4(e) cannot be detected because the l/d value is 0.233, which is smaller than 0.25.

3. Experimental Investigations

3.1. Test Specimen and Instruments. An experimental investigation was conducted to study whether the IE method could be used to detect the voids in grouted lap-splice connections in a precast shear wall. The dimensions of the specimen are shown in Table 1. Details of the specimen can be found in Figure 5. There are 18 typical grouting holes in the specimen with 9 holes (i.e., hole A through I) at each test surface (i.e., test surfaces 1 and 2). Here, the conditions of holes A, B, C, G, H, and I at test surface 1 were the same as test surface 2. Hole A consisted of solid grout with steel bars. Hole B consisted of only solid grout. Hole C had no grout but had steel bars. Holes G, H, and I consisted of defective grout and steel bars. Plastic foam was used to form defects of 10%, 20%, and 30% of the hole volume. Holes D, E, and F at test surface 1 had defects of 10%, 20%, and 30%, respectively, whereas at test surface 2, they were all solid grout with steel bars. A test on solid concrete of the shear wall was also conducted for reference. Therefore, a total of 10 test conditions were considered in this study.

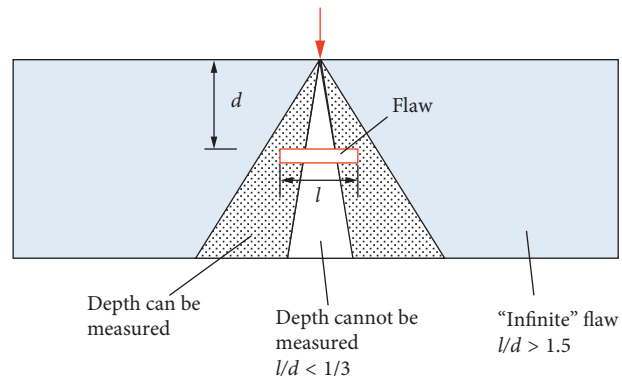

Figure 3: Smallest detectable horizontal crack or void [1] (l = length of flaw; d = depth of flaw).

The IE test system used in this study was SPC-MATS developed by Sichuan Central Inspection Technology Inc. as shown in Figure 6. A sampling frequency of 500 kHz and length of 4,096 points were used to capture the waveforms, for a record length of 8.192 ms. The frequency resolution in the computed amplitude spectra was 0.122 kHz. A steel ball with a diameter of 6 mm was used for impact. A piezoelectric accelerometer produced by Fuji Ceramics Corporation with a working frequency up to 15 kHz was adopted, and the electronic signals amplified were transferred into the digital signals through data acquisition and processing module. The test lines were arranged on both sides, directly above the holes. As shown in Figure 7, the measuring points were arranged at intervals of 40 mm along the test line direction. The distance between the impact point and the receiver location was between 20 and 30 mm. There are 20 testing points along each hole; Points 1–15 are located directly over the hole, and Points 16–20 are located in the solid part to obtain the solid thickness frequency.

3.2. Test Results. Figures 8(a)–8(j) illustrate examples of the waveforms and amplitude spectra of the 10 test conditions. Each figure represents one impact, and it should be mentioned that the results obtained from different impacts at one point remained almost the same. In Figure 8(j), it can be seen that the measured peak frequency of the solid wall (9.644 kHz) agrees well with the calculated value (9.50 kHz) using equation (1) while the V_p is 3960 m/s. The test results obtained from Hole A were the same as the solid concrete

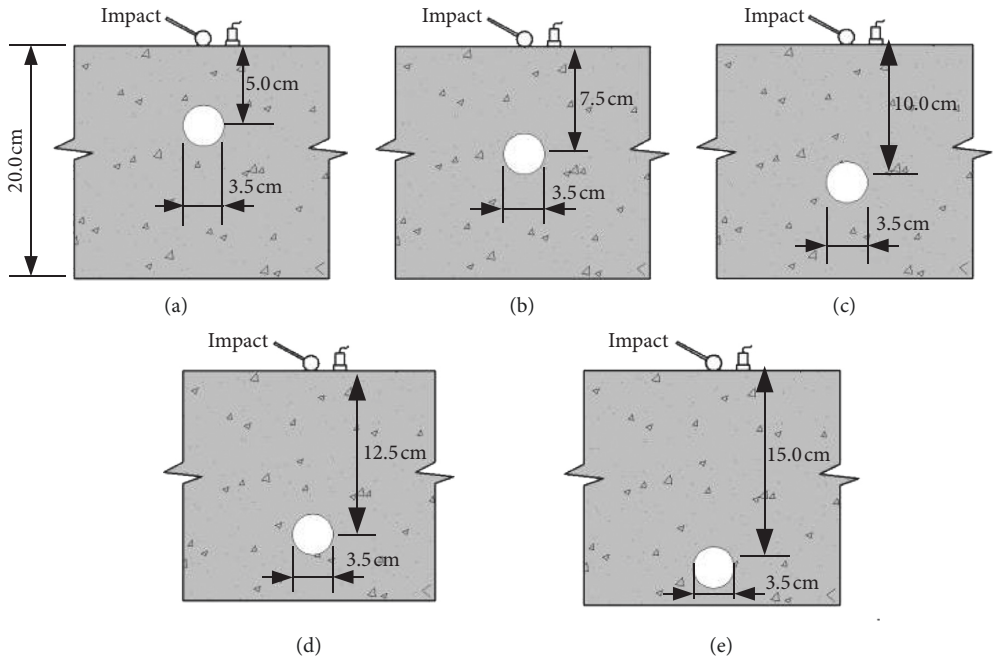

Figure 4: Ratios of the lateral dimension and depths of a 35 mm hole. (a) $l/d = 0.7$. (b) $l/d = 0.467$. (c) $l/d = 0.35$. (d) $l/d = 0.28$. (e) $l/d = 0.233$.

Table 1: Details of the specimen.

Dimension (mm)	Diameter of hole (mm)	Hole length (mm)	Diameter of steel bar (mm)	Anchorage length of steel bar (mm)	h_g (mm)
$2000 \times 1000 \times 200$	35	630	16	600	30

Note. h_g is the constructional measure height (see Figure 1), which is equal to the diameter of the grouting outlet hole in this study.

condition, including the time-history response and the frequency response, indicating that the hole A behaved as a solid infill material. For holes with grout defects, the predominant frequency did not change until a considerable defect occurred (i.e., hole F, H, and I). The empty hole C presented the lowest predominant frequency due to the hole (Figure 8(c)). This was because the propagation path of the stress wave was the longest due to no grout in the hole, which produced a longer travel time. Also, it should be mentioned that Figure 8(c) shows only one peak in the amplitude spectrum although two holes existed, which is because the frequency corresponding to the depth of the nearest hole was beyond the measuring range of the instrument. In addition, for some holes (e.g., Figure 8(e)), the obtained frequency might not indicate a defect although it was theoretically detectable, owing to the limited defect size compared with the size of the whole specimen. Taken together, the predominant frequency decreased with the increase of the void in the grout, indicating that the IE method offers the potential to detect defects in grouted lap-splice connections in precast shear walls.

In order to facilitate an in-depth understanding on the performance of IE method, the peak frequency obtained at each measuring point along each hole are shown in Figure 9, in which "–1" and "–2" represent results obtained at test surfaces 1 and 2, respectively. For hole A, the peak frequency values at the measuring points 1–15 were almost equal to the values at measuring points 16–20 (i.e., around 9.644 kHz), although slight scatter existed at some measuring points on surface 1 and they were also equal to the frequency values of hole B. These results indicate that the fully grouted holes behaved as solid concrete and the bars did not affect the obtained frequency value. However, for empty hole C, the peak frequencies at measuring points 1–15 were obviously lower than those at measuring points 16–20. Due to no grouting inside hole C, the propagation path of the stress wave increased, which decreased at the obtained peak frequency.

For hole G (10% void), the peak frequencies at measuring points 1–15 were slightly inferior to 9.644 kHz. However, the peak frequencies for holes H (20% void) and I (30% void) were as low as 9.277 kHz, which indicates that with the increase of the defect, the peak frequency would be reduced. Similar observations can be seen for holes D, E, and F. Here, it should be noted that the depth of the defect could not be discerned because the shifted frequency values were almost equal for the two test surfaces. However, the test results indicated that the IE method offered a good potential to indicate the relative level of the defect in the grouted lap-splice connections.

4. Finite Element Analysis

Two dimensional (2D) finite element (FE) analyses [19–21] based on the general purpose FE software ABAQUS were

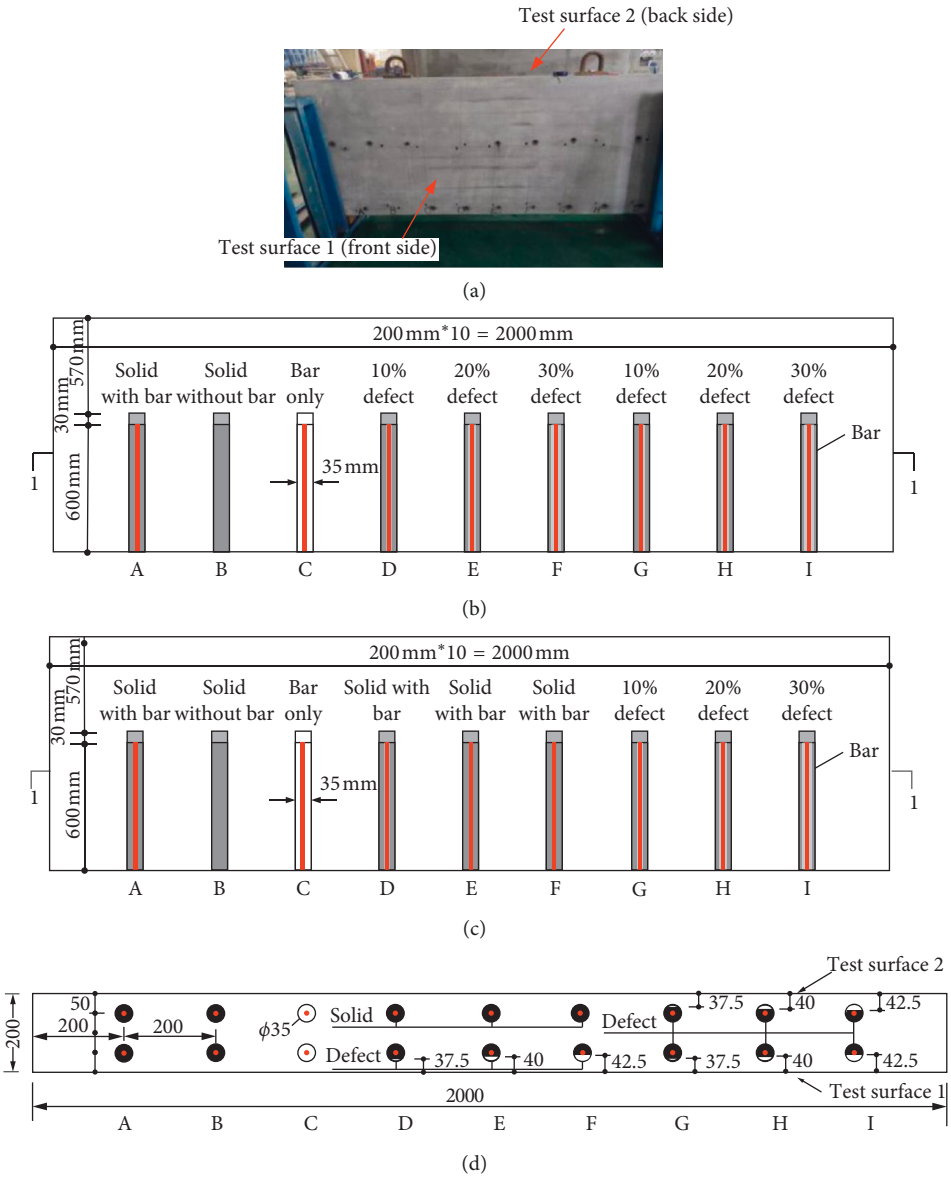

Figure 5: Details of the shear wall test specimen. (a) Photo of the test specimen. (b) Details of test surface 1. (c) Details of test surface 2. (d) Section 1-1.

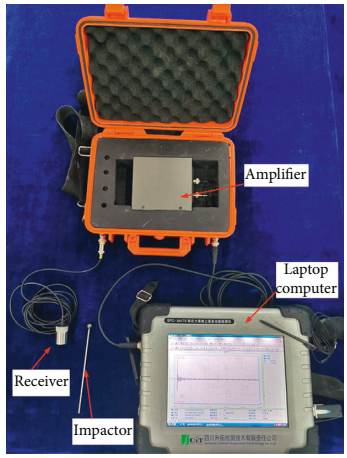

Figure 6: Instruments for IE test.

used to simulate the IE test. After a working model was developed, a parametric study was conducted to investigate the effect of the hole depth on the peak frequency in the amplitude spectrum. Details of the FE model, the comparison between test and analytical results, and the parametric study results are presented in this section.

4.1. General Description. The view of the whole model is shown in Figure 10. Plane strain elements were used for modeling the concrete and the grout. In the model, perfect bond was assumed between concrete and grout (i.e., the "TIE" command in ABAQUS was used). In order to simulate the different defect levels, the grout shape was defined according the sectional view in Figure 5(d). The impact point is set above the defect, and the recording point is set 3 cm away from the

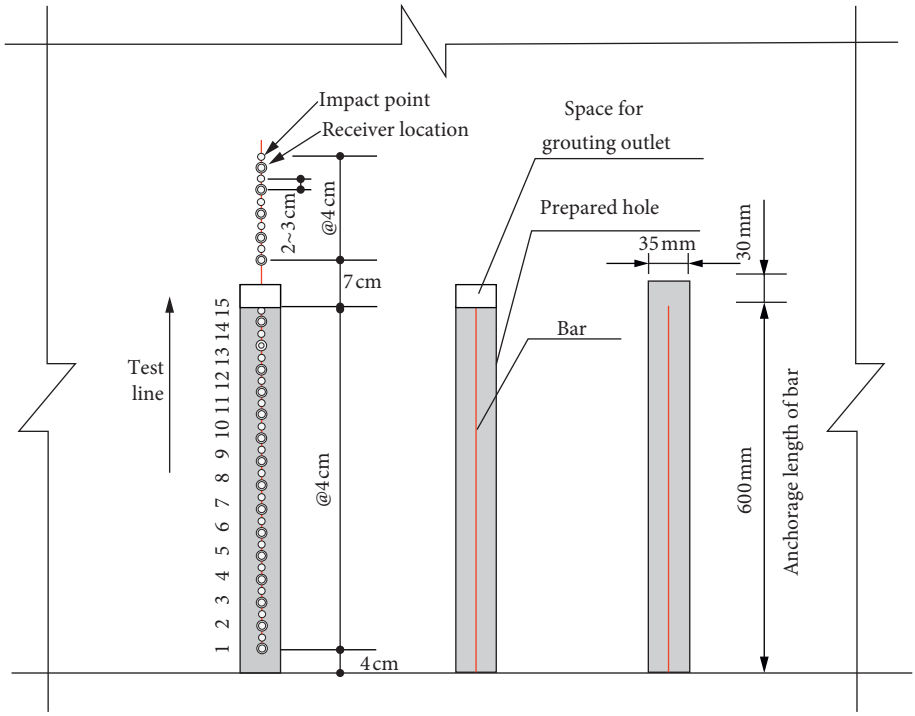

Figure 7: Test scheme.

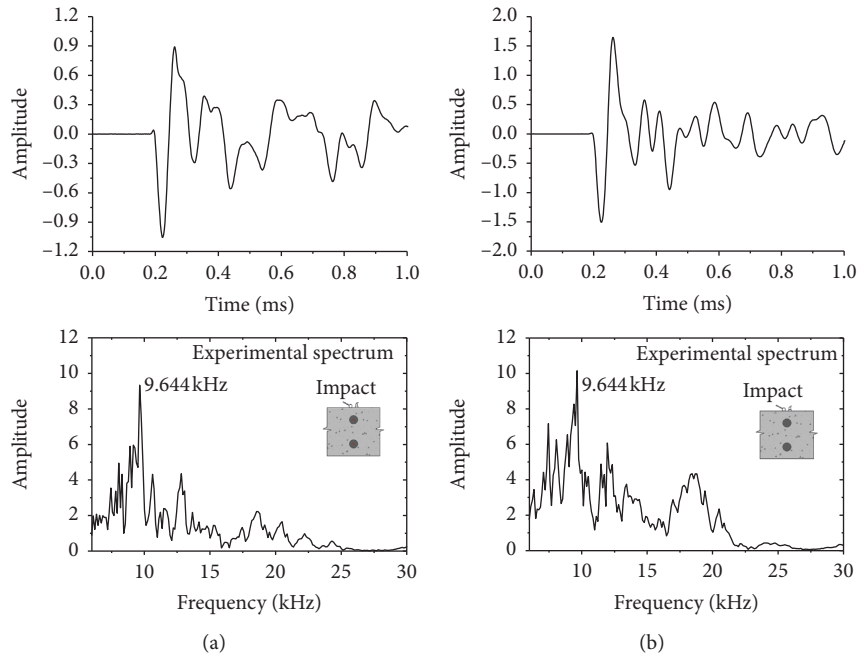

Figure 8: Continued.

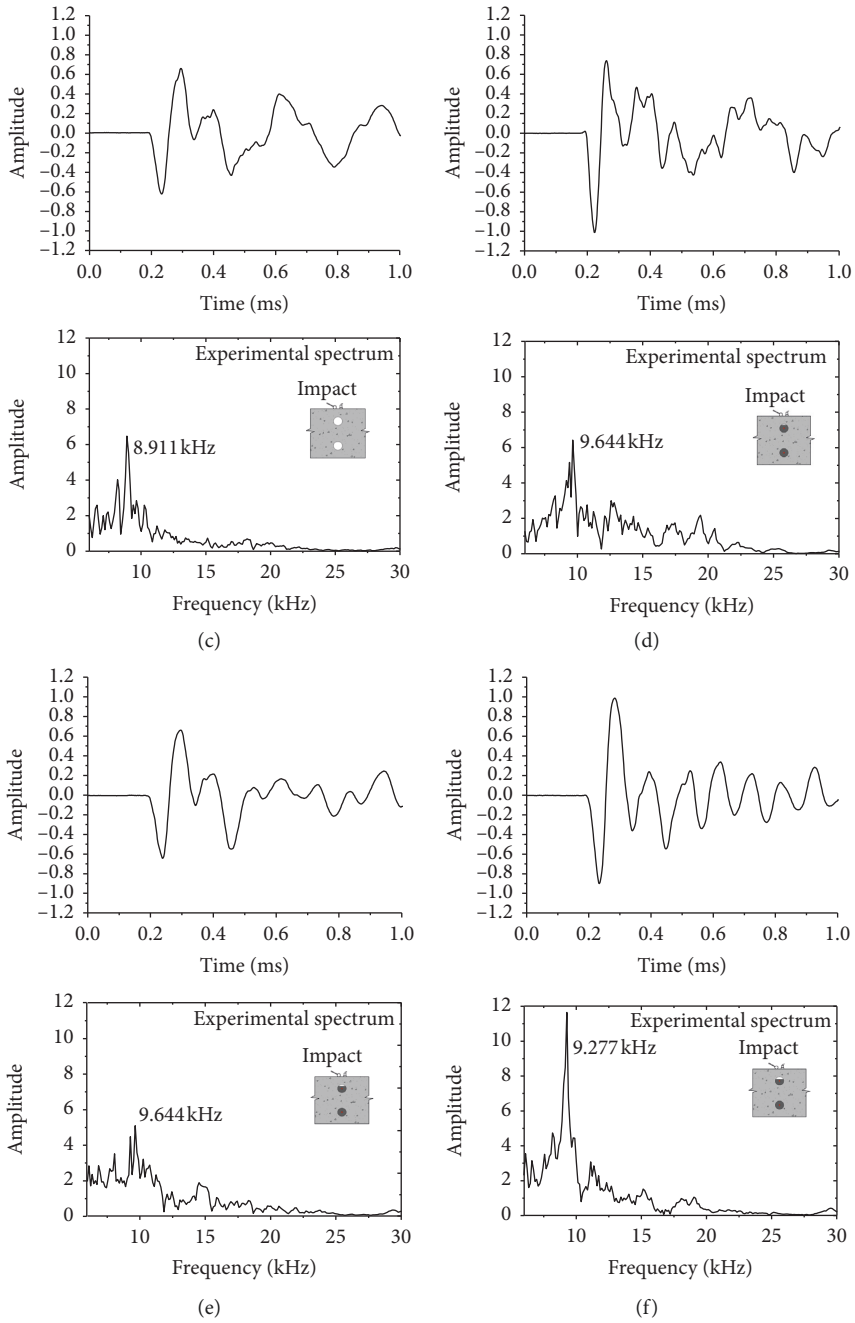

Figure 8: Continued.

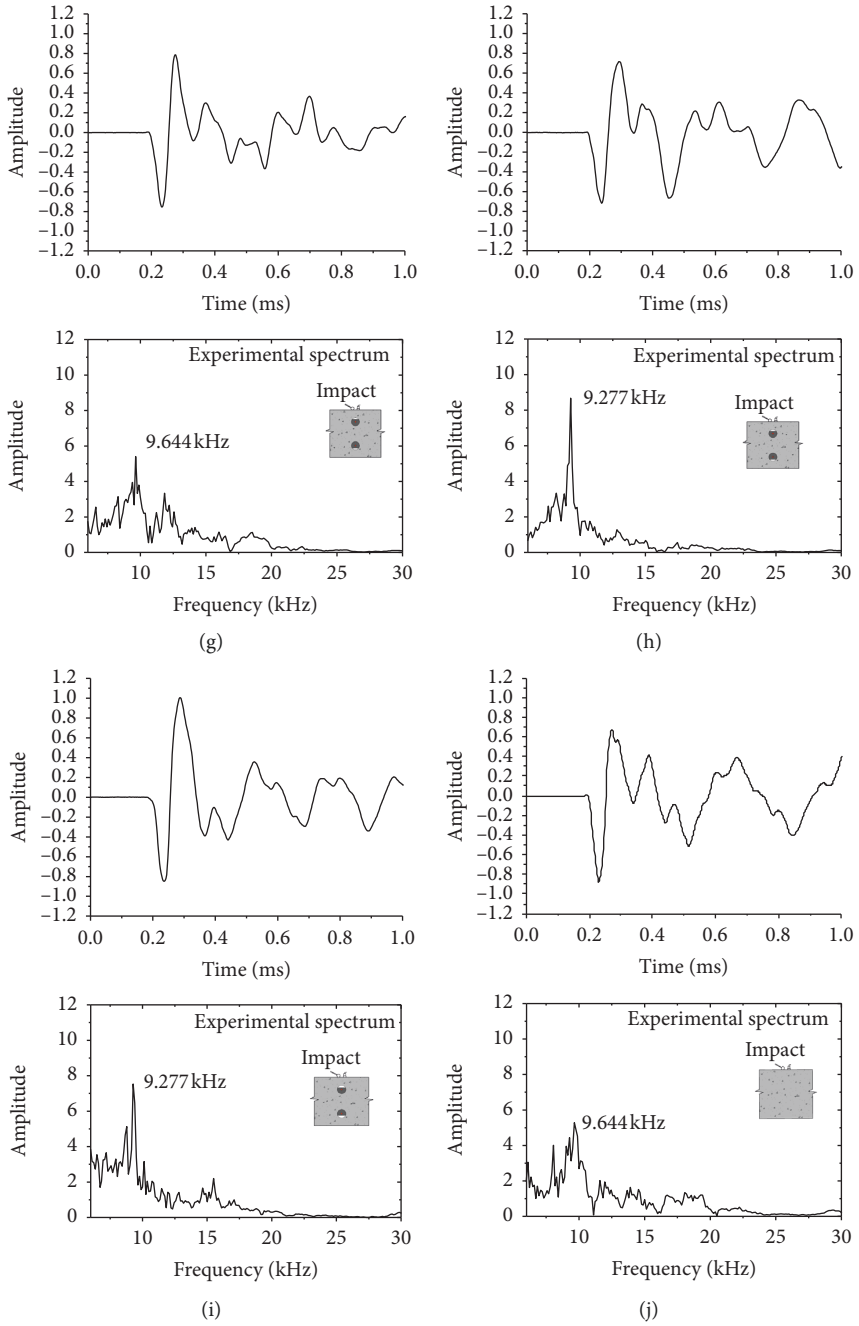

Figure 8: Waveforms and amplitude spectra obtained under different conditions. (a) Solid grout with reinforcement (hole A). (b) Solid grout without reinforcement (hole B). (c) Ungrouted (hole C). (d) Grout defect 10% at test surface 1 (hole D). (e) Grout defect 20% at test surface 1 (hole E). (f) Grout defect 30% at test surface 1 (hole F). (g) Grout defect 10% at test surfaces 1 and 2 (hole G). (h) Grout defect 20% at test surfaces 1 and 2 (hole H). (i) Grout defect 30% at test surfaces 1 and 2 (hole I). (j) Solid concrete (hole J).

impact point. The material properties of the concrete and grout are shown in Table 2. In order to ensure the accuracy of the FE analysis, the element size was set as 5 mm [2]. The explicit dynamic analysis method was used. The impact duration was 25 μs. A load value of 5 N was adopted in the analysis. The time-history of the impact force is assumed to be a half sine curve. The record length is 6 ms with the sampling frequency of 500 kHz. The translation degrees of freedom at the left and right edges of the models in Figure 10 were fixed.

4.2. Comparison between Test and Analysis Results. Figure 11 shows the propagation of stress waves in the model under impact loading. After the analysis was completed, the peak frequency values from the test and analytical results were compared as shown in Table 3. It can be seen from the table that the analytical results agreed well with the test results. The experimental wave speed in solid part of the wall, which was calculated to be 4020 m/s by equation (1), was slightly higher than the value of 3960 m/s used in the model. The maximum

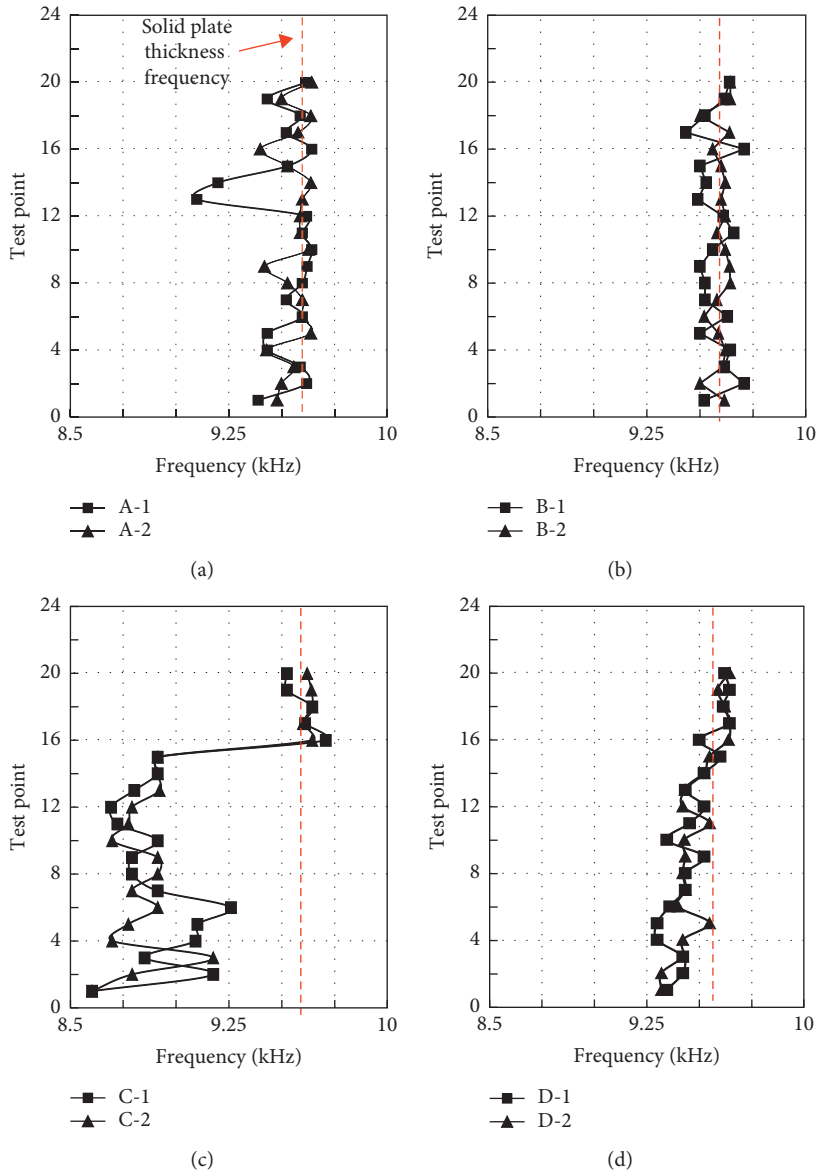

Figure 9: Continued.

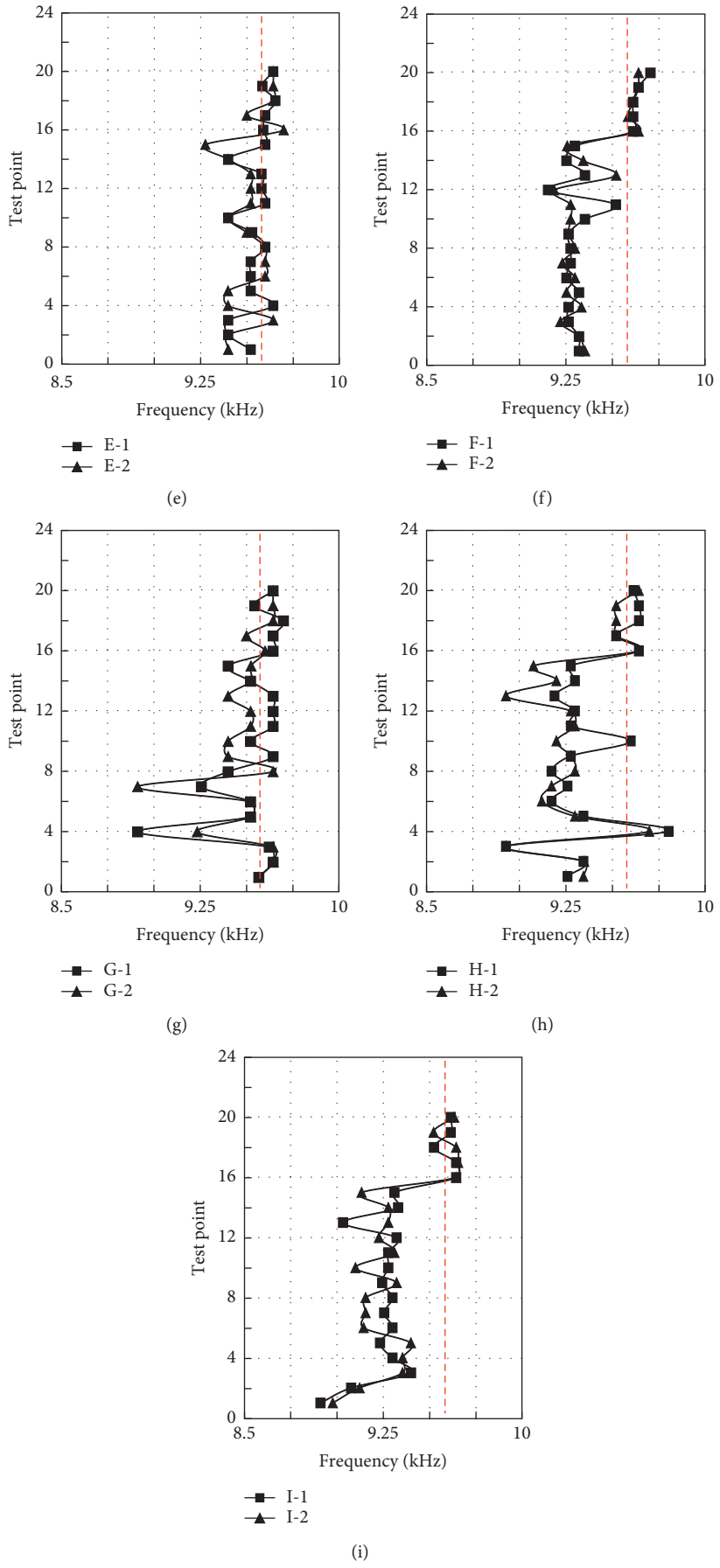

Figure 9: Test results of all holes in the specimen. (a) Hole A (solid). (b) Hole B (solid). (c) Hole C (empty). (d) Hole D (10%-solid). (e) Hole E (20%-solid). (f) Hole F (30%-solid). (g) Hole G (10%). (h) Hole H (20%). (i) Hole I (30%).

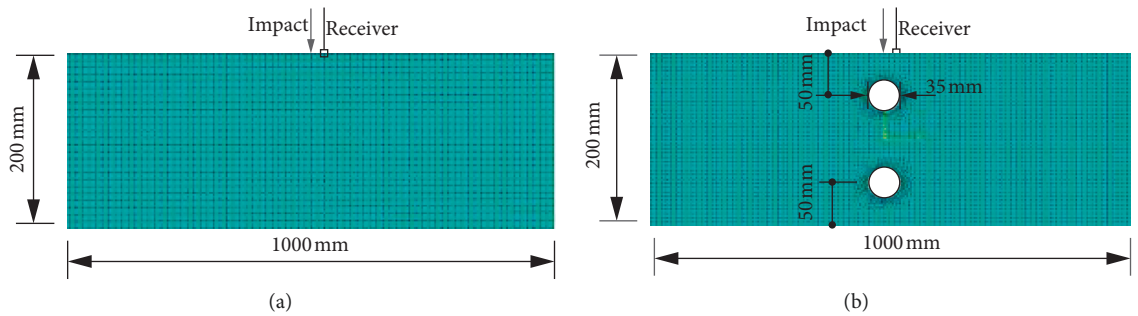

Figure 10: Details of the 2-D finite element model. (a) Solid specimen. (b) Hole in the specimen.

Table 2: Material properties.

Material	Mass density (kg/m^3)	Young's modulus (GPa)	Poisson's ratio	V_p (m/s)
Concrete	2440	34.5	0.2	3960
Grout	2500	33.0	0.2	3830

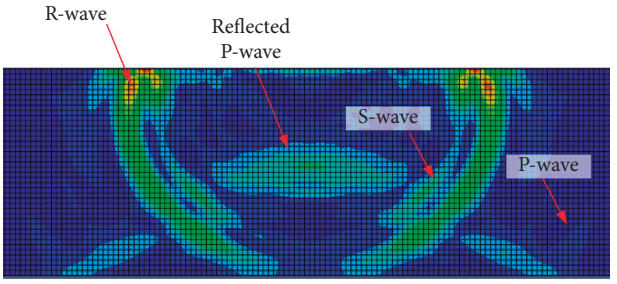

Figure 11: Wave propagation simulation.

Table 3: Comparison of experimental and analytical results.

Conditions	Defect ratio (%)	FE analysis frequency value (kHz)	Experimental frequency value (kHz)	Error (%)
Hole A and B	0	9.497	9.644	1.52
Hole D	10	9.497	9.644	1.52
Hole E	20	9.330	9.277	0.57
Hole F	30	9.330	9.277	0.57
Hole G	10	9.497	9.644	1.52
Hole H	20	9.330	9.277	0.57
Hole I	30	9.163	8.911	2.83
Hole C	100	8.997	8.911	0.97

error between the experimental and analytical frequencies was 2.83%. In the FE analysis, the ratio of frequency between hole C (empty) and hole A (solid) was 0.947, which is similar to the experimental value of 0.924. The higher value for the experimental peak frequency for the solid wall means that the actual concrete had a slightly higher wave speed than used in the FE model. These observations indicated that the FE model could be used for modelling the frequency response of grouted lap-splice connections in the walls.

4.3. Parametric Analysis. Based on the validated model, a parametric study was conducted to investigate the effect of the depth of an empty hole on the peak frequency response in the amplitude spectrum. A total of five depths were considered: 50, 75, 100, 125, and 150 mm. The hole diameter was 35 mm, and the thickness of the wall was 200 mm. The element size, boundary conditions, and material properties remained the same as the model mentioned above.

The amplitude spectrums for the different hole depths are shown in Figure 12. The peak frequency (f_1), the frequency based on the reflection of hole (f_2), the corresponding amplitude, and the back-calculated depth by equation (1) are summarized in Table 4. Here, the wave path regarding f_1 and f_2 can be seen in Figure 12(f). It could be seen from the table that the back-calculated depth based on f_2 agreed well with the numerical model. However, the corresponding amplitude of f_2 was lower (See Figures 12(a)–12(e)) and it was hard to be obtained in engineering practice. In addition, the mode frequencies of the specimen can be seen in the frequency

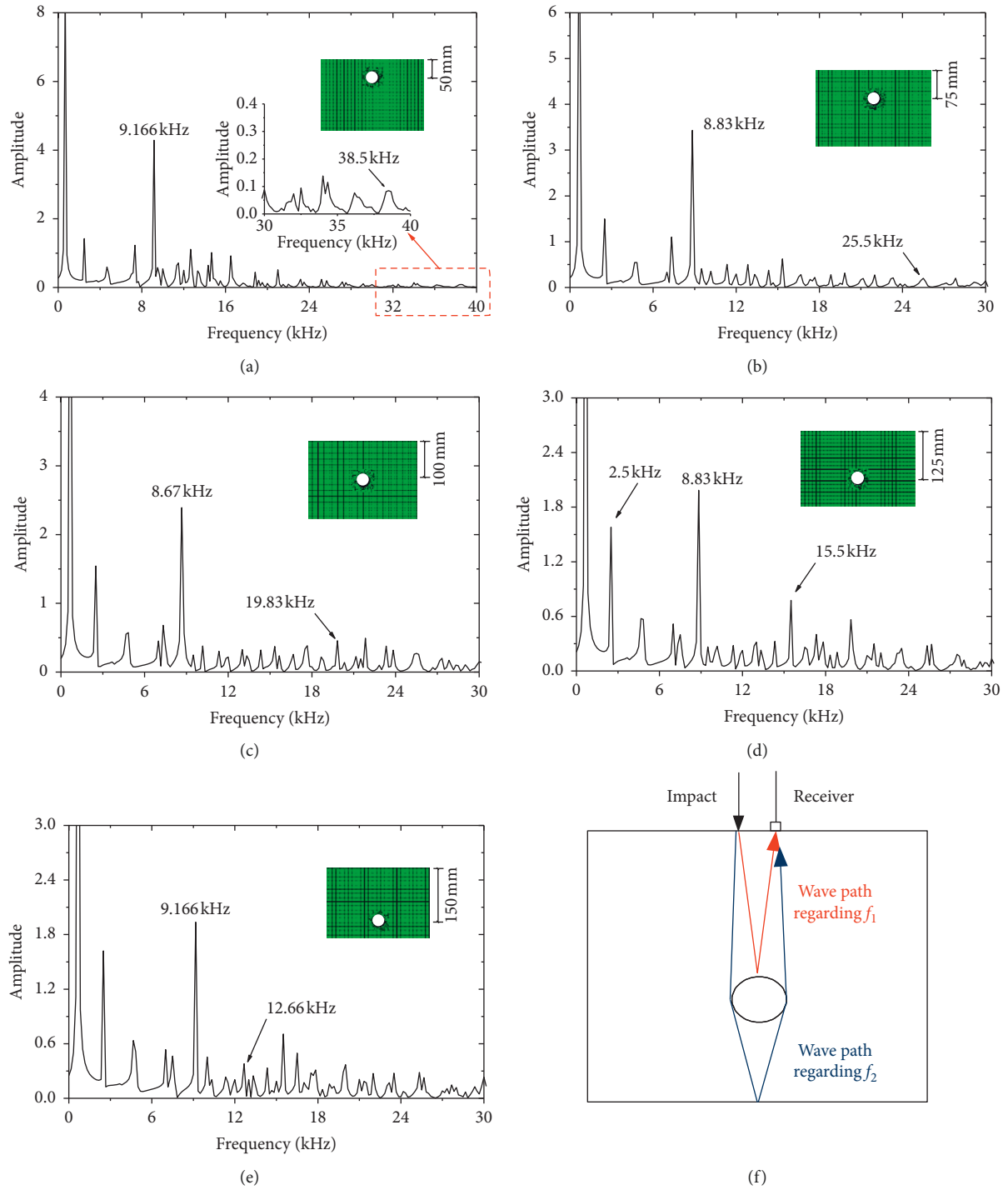

Figure 12: Corresponding frequencies of different depths of hole. (a) 50 mm. (b) 75 mm. (c) 100 mm. (d) 125 mm. (e) 150 mm. (f) Wave path.

spectrum. For example, in Figure 12(d), the peak value of 2.5 kHz was the ninth mode frequency of the specimen.

The relationships between f_1, the corresponding amplitudes and hole depth are summarized in Figure 13. It can be seen that as the hole depth increased, the peak frequency value initially decreased with depth until the hole was at the midthickness of the wall. Then, the frequency increased with increasing depth. The response was symmetrical. However, the amplitude of the frequency peak decreased with increasing depth of the hole. This observation might help to further clarify the location of the void since the signal of f_1 was easy to obtain in engineering practice, which is essential in precast shear wall flaw detecting. However, it should be mentioned that the calibration was probably required to facilitate an accurate amplitude in test.

Table 4: Results of parametric analysis.

Buried depth (mm)	50	75	100	125	150
f_1 (kHz)	9.166	8.83	8.66	8.83	9.166
Amplitude (10^{-8})	4.48	3.45	2.37	2.00	1.93
Back-calculated depth based on f_1 (mm)	207.38	215.27	219.42	215.27	207.38
f_2 (kHz)	38.50	25.50	19.83	15.50	12.66
Amplitude (10^{-8})	0.08	0.19	0.45	0.78	0.38
Back-calculated depth based on f_2 (mm)	49.37	74.54	95.85	122.60	150.14

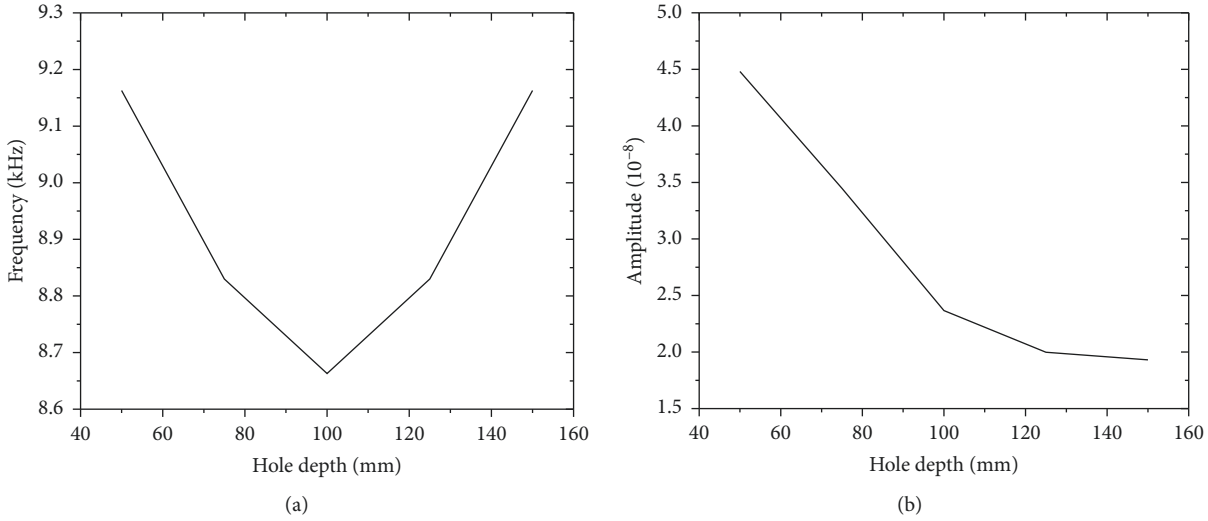

Figure 13: Relationships between frequency, amplitude and hole depth. (a) Relationship between frequency and hole depth. (b) Relationship between amplitude and hole depth.

5. Conclusions

This study was mainly focused on investigating the feasibility of the impact-echo (IE) method in detecting defects in grouted lap-splice connections in precast walls. To this end, experimental investigations were conducted firstly. Eighteen grouting holes with different levels of artificial defects were prepared in a shear wall specimen, and the IE method was used to obtain the frequency response data. In addition, finite element (FE) analyses were conducted to simulate the IE test, and a parametric study was conducted to investigate the effect of the depth of an empty hole on the peak frequency value and its amplitude. The results obtained in this study allowed the following conclusions to be drawn:

(1) The presence of a defect in the grout is indicated by a shift in the solid plate thickness frequency to a lower value. Based on the test results, the IE method demonstrated a good potential to detect grouting defects and could even provide a qualitative indication the defect level in grouted lap-splice connections.

(2) The proposed FE model was confirmed to be suitable to simulate the dynamic response of the wall with grouting holes based on the comparison between test and analysis results.

(3) Based on the parametric study, as the hole depth increased, the peak frequency decreased to a minimum value with the hole at the middle of the wall and then increased in a symmetric manner. The amplitude decreased continuously with increasing depth.

(4) The parametric study also indicated that frequency shift to a lower value cannot be used as an indicator of the depth of the defect in engineering practice.

This study adopted a steel ball with a diameter of 6 mm used as impactor and an acceleration sensor, whereas those facilities are hard to catch high frequency response. In further study, different types of the facilities (e.g., tiny steel ball with conical displacement transducer) suitable for detecting the shallow defects discussed in this study will be adopted to validate the application of the IE method in grouting defect detection. In addition, in order to estimate the depth of the defect from the amplitude spectrum, a calibration on the obtained signal amplitude might be required in the future.

Data Availability

The data used to support the findings of this study are included within the article.

Conflicts of Interest

The authors declare that there are no conflicts of interest regarding the publication of this paper.

Acknowledgments

The authors appreciate the financial support from the National Key Research and Development Program of China (2016YFC0701802, 2016YFC0701507, and 2011BAJ03B04) and Anhui Provincial Natural Science Foundation (1908085ME144). In addition, the following companies are gratefully acknowledged for their material donations and assistance to the project: Anhui Hailong Construction Industry Co., LTD, and Shenzhen Modern Construction Technology Co. LTD.

References

[1] N. J. Carino, "The impact-echo method: an overview," in *Proceedings of the 2001 Structures Congress and Exposition*, Washington, DC, USA, National Advances in Nondestructive Testing, 12th edition, May 2001.

[2] M. Sansalone and W. B. Streett, *Impact-Echo: Nondestructive Testing of Concrete and Masonry*, Bullbrier Press, Ithaca, NY, USA, 1997.

[3] F. Schubert and B. Köhler, "Ten lectures on impact-echo," *Journal of Nondestructive Evaluation*, vol. 27, no. 1–3, pp. 5–21, 2008.

[4] F. Schubert, H. Wiggenhauser, and R. Lausch, "On the accuracy of thickness measurements in impact-echo testing of finite concrete specimens––numerical and experimental results," *Ultrasonics*, vol. 42, no. 1–9, pp. 897–901, 2004.

[5] A. Gibson and J. S. Popovics, "Lamb wave basis for impact-echo method analysis," *Journal of Engineering Mechanics*, vol. 131, no. 4, pp. 438–443, 2005.

[6] O. Baggens and N. Ryden, "Systematic errors in impact-echo thickness estimation due to near field effects," *NDT & E International*, vol. 69, pp. 16–27, 2015.

[7] Y. Lin and M. Sansalone, "Detecting flaws in concrete beams and columns using the impact-echo method," *ACI Materials Journal*, vol. 89, no. 4, 1992.

[8] C. Hsiao, C.-C. Cheng, T. Liou, and Y. Juang, "Detecting flaws in concrete blocks using the impact-echo method," *NDT & E International*, vol. 41, no. 2, pp. 98–107, 2008.

[9] C.-T. Hsieh and Y. Lin, "Detecting debonding flaws at the epoxy-concrete interfaces in near-surface mounted CFRP strengthening beams using the impact-echo method," *NDT & E International*, vol. 83, no. 3, pp. 1–13, 2016.

[10] W. F. Tawhed and S. L. Gassman, "Damage assessment of concrete bridge decks using Impact-Echo method," *ACI Material Journal*, vol. 99, no. 3, 2002.

[11] Y. Lin and K.-L. Lin, "Transient impact response of bridge i-girders with and without flaws," *Journal of Bridge Engineering*, vol. 2, no. 4, pp. 131–138, 1997.

[12] D. G. Aggelis, T. Shiotani, and K. Kasai, "Evaluation of grouting in tunnel lining using impact-echo," *Tunnelling and Underground Space Technology*, vol. 23, no. 6, pp. 629–637, 2008.

[13] J. M. Kang, S. Song, D. Park, and C. Choi, "Detection of cavities around concrete sewage pipelines using impact-echo method," *Tunnelling and Underground Space Technology*, vol. 65, pp. 1–11, 2017.

[14] M. T. A. Chaudhary, "Effectiveness of impact echo testing in detecting flaws in prestressed concrete slabs," *Construction and Building Materials*, vol. 47, pp. 753–759, 2013.

[15] M. Sansalone and N. J. Carino, "Detecting honeycombing, the depth of surface-opening cracks, and ungrouted ducts using the impact-echo method," *Concrete International*, vol. 10, no. 4, 1988.

[16] N. J. Carino and M. Sansalone, "Detecting voids in grouted ducts using the impact-echo method," *ACI Materials Journal*, vol. 89, no. 3, 1992.

[17] B. J. Jaeger, M. J. Sansalone, and R. W. Poston, "Detecting voids in grouted tendon ducts of post-tensioned concrete structures using the Impact Echo Method," *ACI Structural Journal*, vol. 93, no. 4, 1996.

[18] R. Muldoon, A. Chalker, M. C. Forde, M. Ohtsu, and F. Kunisue, "Identifying voids in plastic ducts in post-tensioning prestressed concrete members by resonant frequency of impact-echo, SIBIE and tomography," *Construction and Building Materials*, vol. 21, no. 3, pp. 527–537, 2007.

[19] M. Sansalone, N. J. Carino, and N. N. Hsu, "A finite element study of transient wave propagation in plates," *Journal of Research of the National Bureau of Standards*, vol. 92, no. 4, pp. 267–278, 1987.

[20] M. Sansalone, N. J. Carino, and N. N. Hsu, "A finite element study of the interaction of transient stress waves with planar flaws," *Journal of Research of the National Bureau of Standards*, vol. 92, no. 4, pp. 279–290, 1987.

[21] M. Hill, J. Mchugh, and J. D. Turner, "Cross-sectional modes in impact-echo testing of concrete structures," *Journal of Structural Engineering*, vol. 126, no. 2, pp. 228–234, 2000.